Applied Physics Letters

Effect of the magnetic film thickness on the enhancement of the spin current by multi-magnon processes

O. Dzyapko, H. Kurebayashi, V. E. Demidov, M. Evelt, A. J. Ferguson et al.

Citation: Appl. Phys. Lett. **102**, 252409 (2013); doi: 10.1063/1.4812812
View online: http://dx.doi.org/10.1063/1.4812812
View Table of Contents: http://apl.aip.org/resource/1/APPLAB/v102/i25
Published by the AIP Publishing LLC.

APPLIED PHYSICS LETTERS **102**, 252409 (2013)

Effect of the magnetic film thickness on the enhancement of the spin current by multi-magnon processes

O. Dzyapko,[1,a)] H. Kurebayashi,[2,3] V. E. Demidov,[1] M. Evelt,[1] A. J. Ferguson,[2] and S. O. Demokritov[1]
[1]*Institute for Applied Physics and Center for Nonlinear Science, University of Muenster, Corrensstrasse 2-4, 48149 Muenster, Germany*
[2]*Cavendish Laboratory, University of Cambridge, J. J. Thomson Avenue, Cambridge CB3 0HE, United Kingdom*
[3]*PRESTO, Japan Science and Technology Agency, Kawaguchi 332-0012, Japan*

(Received 18 April 2013; accepted 16 June 2013; published online 28 June 2013)

We study experimentally the spin-current generation in yttrium iron garnet (YIG)/Pt bilayers based on YIG films with different thicknesses. Our results show that for all films with thicknesses exceeding a certain value, the spin current in the YIG/Pt system is enhanced at low frequencies. The cut-off frequencies, at which the enhancement starts, as well as the efficiency of the enhancement were found to increase with increasing film thickness. Good correlation between the cut-off frequency and the frequency at which the three-magnon splitting becomes allowed was observed. These findings prove that the latter process is responsible for the spin-current enhancement. © *2013 AIP Publishing LLC*. [http://dx.doi.org/10.1063/1.4812812]

Pure spin currents play a growing role in modern spintronics, since the transfer of the spin not associated with the electric current flow enables the efficient control of magnetic dynamics in both conductive and insulating magnetic materials.[1–11] In particular, the use of pure spin currents was found to allow an electric control of the effective magnetic dynamic damping,[1–3] reduction of high-frequency magnetic noise,[4] excitation and amplification of propagating spin waves,[5–7] stimulation of nonlinear phenomena,[8] and generation of coherent magnetic oscillations.[9–11] Based on these findings, development of a wide class of spintronic devices, comprising conductive and insulating materials is very likely.

Usually, the generation of the spin current in spintronic devices operating with pure spin currents takes place in nonmagnetic conducting materials with strong spin-orbit coupling, such as Pt due to the spin Hall effect (SHE).[12,13] The created spin current is injected into adjacent (conducting or insulating) ferromagnetic layer. From the physical point of view, the spin current is created as a result of triggering a flow of the angular momentum from the lattice of the nonmagnetic material. Since the lattice represents an ideal source of the angular momentum, the utilization of this phenomenon is a promising root for the development of advanced spintronic devices.

A dynamic approach for triggering the angular momentum flow from the lattice was recently demonstrated[14] in a magnetic layer. It was reported that in an yttrium iron garnet (YIG) film, in which a ferromagnetic resonance (FMR) is excited, the transfer of the angular momentum from the lattice causes an enhancement of the spin current injected from YIG into an adjacent Pt layer. It was asserted that the physical mechanism responsible for this transfer is the three-magnon splitting process—the process of splitting of a magnon into two magnons of half frequency, as follows from the energy conservation law. For splitting of the FMR mode, this process is allowed below a given magnetic field (or a given FMR frequency), since for higher field there is no magnon states at frequencies equal to one-half of the FMR frequency. However, even if the process is allowed from the energy conservation law, the total angular momentum of the created magnons is usually not equal to that of the initial magnon. Therefore, to fulfill the angular momentum conservation, this process requires a mixing of the angular momentum of the lattice with that of the magnon system via the magneto-dipole interaction. It is important to note, that in contrast to SHE, the above approach takes advantage of the process in the magnetic layer and, in principle, does not require the presence of an additional nonmagnetic layer with a strong spin-orbit coupling. In fact, the Pt layer in the above studies played the role of the spin-current detector only. Since the first observation of this phenomenon in Ref. 14, the enhancement of the spin current has been confirmed in other studies.[15–17] However, the experiments in Ref. 17 were performed using a YIG film with the thickness of 200 nm, where the three-magnon splitting of the FMR is not allowed, because the magnon spectrum in such thin films does not have available magnon states at frequencies equal to one-half of the FMR frequency at any applied field. Thus, the connection between the angular momentum flow and the three-magnon splitting was questioned in Ref. 17.

In this letter, we report an experimental study of the enhancement of the spin current in YIG/Pt bilayers with different thicknesses of YIG films. We show that the frequencies, at which the enhancement starts, exhibit a clear dependence on the YIG film thickness. Moreover, the enhancement completely vanishes for films with the thickness below a certain value. These findings are in perfect agreement with the theoretical description of the phenomenon based on the three-magnon process. The presented results provide clear evidence that the three-magnon splitting is the actual mechanism responsible for the enhancement of spin current in YIG/Pt systems.

[a)]Author to whom correspondence should be addressed. Electronic mail: dzyapko@uni-muenster.de

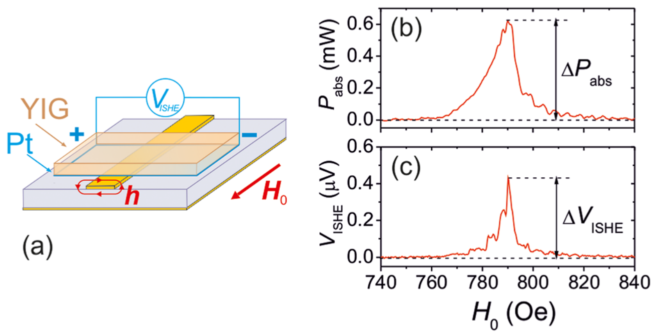

FIG. 1. (a) Schematic of the experiment. (b) Typical curve of the microwave absorption, recoded at $f = 4$ GHz. ΔP_{abs} marks the microwave power absorbed by the FMR mode. (c) Field dependence of the ISHE voltage obtained under the same conditions, as the absorption curve in (b). ΔV_{ISHE} marks the value of the voltage at FMR conditions.

The schematic of the experiment is shown in Fig. 1(a). The studied samples are single crystalline YIG films grown by liquid phase epitaxy with a Pt film deposited on top of the YIG by the magnetron sputtering. The thicknesses of the studied YIG films were $d = 0.8$, 3.1, 5.1, and 6 μm and that of the Pt layer was 15 nm. The lateral sizes of the samples were 1.5 by 6 mm. As in the previous studies,[14] in our experiments, we used stripline FMR technique, since it allows measurements in the wide frequency range. The samples were attached to the standard 50 Ohm microwave microstrip transmission line with the width of 0.5 mm with the long sample side perpendicular to the line. A microwave signal with the carrier frequency f in the range between 2 and 5 GHz was applied to the input of the transmission line. The microwave power absorbed by the sample P_{abs} was monitored by detecting the transmitted power at the output of the line and that reflected from the input of the test device by using calibrated semiconductor microwave detectors. The device was placed into a static magnetic field H_0, applied parallel to the transmission line to achieve maximum efficiency of the FMR excitation, which requires the dynamic magnetic field produced by the microwave current to be perpendicular to H_0.

By keeping the frequency of the excitation signal constant and varying the static magnetic field, we recorded curves of the microwave absorption, as shown in Fig. 1(b) for the case $f = 4$ GHz. The obtained curves exhibit a maximum ΔP_{abs} at a particular H_0 corresponding to the quasi-uniform FMR in the YIG sample. This field was found to vary with the variation of the excitation frequency f in perfect agreement with the Kittel formula.[18] Along with the fundamental FMR mode, higher-order standing spin-wave modes are excited in the film and contribute to the absorption curve,[19] leading to its broadening and asymmetry.

As described in detail in Ref. 14, the excitation of the dynamic magnetization in the YIG film results in the flow of the spin current across the YIG/Pt interface, which can be detected by using the inverse spin Hall effect (ISHE)[20] leading to a voltage V_{ISHE} across the Pt film proportional to the strength of the spin current. V_{ISHE} was measured by means of two electrodes attached at the edges of the Pt film, as shown in Fig. 1(a). To increase the sensitivity of the measurements, the lock-in technique utilizing the modulation of the excitation microwave power at the frequency of 5 kHz was used. Typical dependence of V_{ISHE} on the static magnetic field is shown in Fig. 1(c). As expected, V_{ISHE} also exhibits a maximum ΔV_{ISHE} at the FMR field. Similarly to the microwave absorption curve [Fig. 1(b)], the V_{ISHE} curve is also asymmetric due to the influence of higher-order standing spin-wave modes, although, it shows a slightly different shape because of the variation of the efficiency of the spin-current generation from one mode to the other.

Figure 2(a) illustrates the frequency dependence of the maximal absorbed power ΔP_{abs} and the corresponding ISHE voltage ΔV_{ISHE} characterizing the FMR mode of the film with $d = 5.1$ μm. In agreement with the results of Ref. 14, the generated spin current exhibits an abrupt increase below a given cut-off frequency f_c and, correspondingly, static magnetic field, which was associated with the onset of the three-magnon splitting process triggering an additional flow of the angular momentum from the lattice of the ferromagnetic film into the magnon system. Simultaneously, the absorbed microwave power decreases below f_c. The amount of the absorbed microwave power ΔP_{abs} is proportional to the amplitude of the dynamic magnetization squared m^2: $\Delta P_{abs} \propto \chi'' h^2$, where h is the dynamic magnetic field and χ'' is the imaginary part of the magnetic susceptibility ($\boldsymbol{m} = \overleftrightarrow{\chi}\, \boldsymbol{h}$).[21] On the other hand, the ISHE voltage ΔV_{ISHE} generated by the precession is also proportional to m^2 (see Ref. 22 for detail). Thus, both ΔP_{abs} and ΔV_{ISHE} are proportional to the intensity of the magnetization precession. Therefore, for a given dynamic magnetic mode, for example,

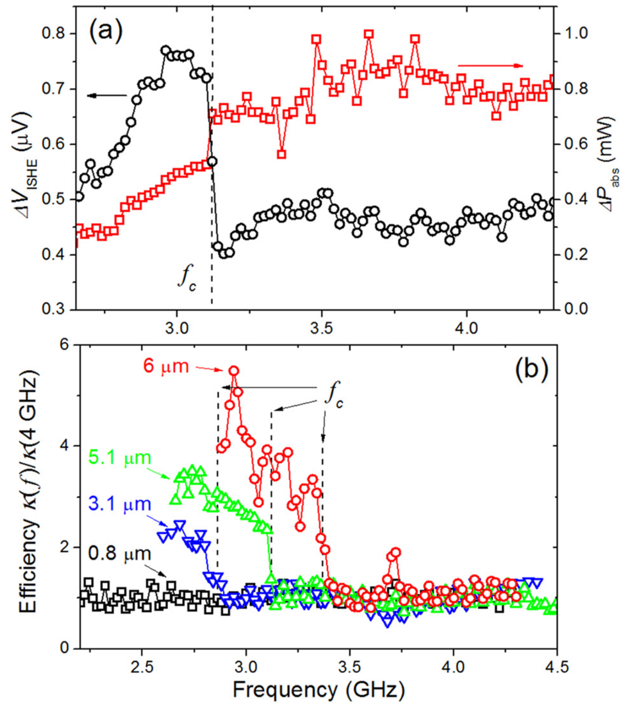

FIG. 2. (a) Frequency dependences of ΔP_{abs} and ΔV_{ISHE} for the quasi-uniform FMR mode for the sample with $d = 5.1$ μm. Note opposite behavior of the voltage and power dependences at the cut-off frequency f_c: although the absorbed power decreases, meaning smaller amplitude of the dynamic magnetization in YIG, the voltage generated by this magnetization increases. (b) The spin-current conversion efficiency coefficients $\kappa = \Delta V_{ISHE}/\Delta P_{abs}$ normalized to their mean values for $f > 4$ GHz for $d = 0.8$, 3.1, 5.1, and 6 μm, respectively. Vertical dashed lines indicate f_c. Note an increase in f_c with increasing d.

quasi-uniform FMR mode, the ratio $\kappa = \Delta V_{ISHE}/\Delta P_{abs}$ would be independent of the excitation frequency, provided the resonant dynamic susceptibility does not significantly change in the used frequency interval.[21] Correspondingly, variation of κ can be used to characterize the efficiency of the spin-current generation by a particular magnetic mode. To study the effect of the magnetic film thickness d on the spin current generation, we obtained the frequency dependences of the spin-current conversion efficiency for the quasi-uniform FMR mode κ for different YIG thickness samples.

Figure 2(b) shows the frequency dependences of κ for samples with $d = 0.8$, 3.1, 5.1, and 6 μm, respectively, normalized to its mean value at $f > 4$ GHz All the dependences except for that for the sample with $d = 0.8$ μm exhibit a clear abrupt increase below the cut-off frequency f_c marked in Fig. 2(b) by vertical dashed lines. It is clearly seen from the experimental data that f_c varies with the YIG thickness, i.e., for films with smaller d the enhancement starts at lower frequencies.

Provided the enhancement of the spin current generation is associated with the onset of the three-magnon splitting, the variation of f_c should be correlated with the variation of the frequency, at which the three-magnon splitting becomes allowed by the energy and momentum conservation laws. Figure 3(a) shows the lowest-energy branch of the spectra of spin waves for YIG films with thicknesses $d = 0.8$, 3.1, and 6 μm calculated for $H = 100$ Oe by using the theory developed in Ref. 23. The point on the dispersion diagram at the frequency f_0 and the zero wavenumber corresponds to the uniform FMR mode. The three-magnon splitting of the magnon of the quasi-uniform FMR mode represents a creation of two magnons with the frequencies $f_0/2$. Correspondingly, this process is only allowed, if there are available spectral states at this frequency. As seen from Fig. 3(a), this is the case for films with $d = 3.1$ and 6 μm, whereas for the film with $d = 0.8$ μm the lowest frequency in the spectrum f_{min} lies above $f_0/2$. When the static magnetic field H_0 is varied, the spin-wave spectrum is shifted in the frequency space and the relation between the frequencies $f_0/2$ and f_{min} changes too. To characterize this change, we plot in Fig. 3(b) the field dependences of the frequency $f_0/2$ and those of the frequency f_{min} for films with $d = 0.8$, 3.1, and 6 μm. From the data of Fig. 3(b), it is clearly seen that for the film with $d = 0.8$ μm, $f_0/2 < f_{min}$ at any H_0, i.e., the three-magnon splitting is completely prohibited in such thin films. In contrast, for films with $d = 3.1$ and 6 μm, the condition $f_0/2 > f_{min}$ necessary for the three-magnon splitting process is satisfied at H_0 smaller than a certain value $H_0 < H_{3m}$. It is also seen that, with the increase in the film thickness, the crossing point is shifted to larger H_0, corresponding to larger cut-off frequencies, in agreement with the experimental data of Fig. 2(b).

Figure 4 shows a quantitative comparison of the experimentally determined cut-off frequencies f_c, at which the enhancement of the spin current starts (filled symbols), with the calculated frequencies f_{3m}, at which the three-magnon splitting becomes allowed (solid line), for films with different thicknesses. From these data, it is seen that these two frequencies show a very good coincidence, which unambiguously proves that the enhancement of the spin current is associated with the three-magnon splitting.

Additionally, inset in Fig. 4 shows the data characterizing the absolute value of the enhancement of the spin current for different thicknesses of the YIG film. The plotted value is the ratio of the conversion efficiency κ at the onset of the three-magnon splitting region (directly below the cut-off frequency f_c) and the efficiency at frequency 4 GHz, at which the

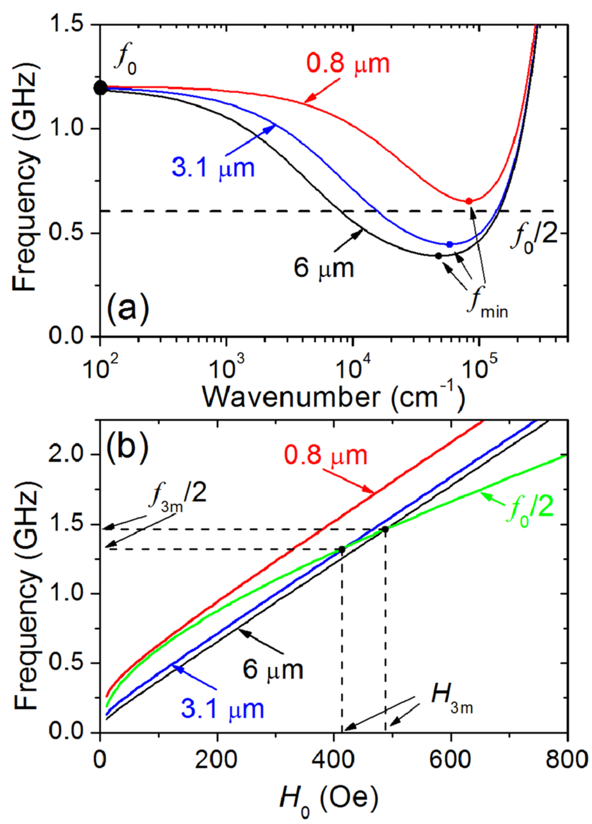

FIG. 3. (a) The lowest-energy branch of the spectra of spin waves for YIG films with thicknesses $d = 0.8$, 3.1, and 6 μm calculated for $H_0 = 100$ Oe (saturation magnetization of YIG $4\pi M_s = 1750$ Gs). The point on the dispersion diagram at the frequency f_0 and the zero wavenumber corresponds to the uniform FMR mode. f_{min} marks the lowest frequency in the spectrum of spin waves. (b) Field dependences of the frequency $f_0/2$ and those of the frequency f_{min} for films with $d = 0.8$, 3.1, and 6 μm. The points of interception determine the onset of the region, where three-magnon splitting is allowed. H_{3m}, f_{3m}—corresponding boundary magnetic field and frequency.

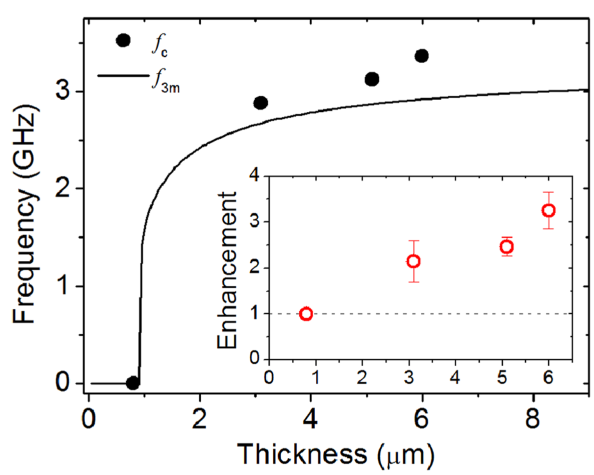

FIG. 4. Comparison of the experimentally determined cut-off frequencies f_c, (symbols), with the calculated frequency, at which the three-magnon splitting becomes allowed f_{3m} (solid line) in films with different thicknesses. Inset: Dependence of the spin-current enhancement strength on the film thickness.

three-magnon splitting is prohibited for all studied films. These data show that the variation of the film thickness also leads to a noticeable variation in the enhancement; with increasing d, the enhancement becomes stronger. This fact clearly shows that the observed enhancement is not connected with modification of the efficiency of the spin-current injection at the YIG/Pt interface, which is solely interfacial process and should be more pronounced for thinner films. Most likely, the observed behaviour of the enhancement strength is associated with the specific features of the absorption of the angular momentum from the lattice in the process of creation of magnons at the frequency $f_0/2$. In fact, the amount of the absorbed angular momentum is equal to the difference of the angular momentum corresponding to the primary magnon of quasi-uniform FMR and that corresponding to the pair of secondary magnons. The latter, in its turn, depends on the contribution of the magneto-dipole interaction to the energy of the secondary magnons: This interaction dominates for magnons with small wavenumber, while at large wavenumbers the exchange interaction plays the dominant role. As seen from Fig. 3(a), with increasing film thickness, the position of the spectral minimum shifts to smaller wavenumbers. Therefore, for thicker films, the effect of the spin-current enhancement due to the momentum flow from the lattice into the magnon system should be more efficient.

In conclusion, the results of the systematic study of the low-frequency enhancement of the spin current in YIG/Pt bilayers provide clear evidence that this enhancement is associated with the onset of three-magnon splitting processes. The obtained results bring us closer to the full understanding of the angular momentum flow in magnetic systems and provide the base for the utilization of the angular momentum control in spintronic devices.

This work was supported in part by the Deutsche Forschungsgemeinschaft. H.K. acknowledges JST for their financial supports.

[1]K. Ando, S. Takahashi, K. Harii, K. Sasage, J. Ieda, S. Maekawa, and E. Saitoh, Phys. Rev. Lett. **101**, 036601 (2008).
[2]L. Liu, T. Moriyama, D. C. Ralph, and R. A. Buhrman, Phys. Rev. Lett. **106**, 036601 (2011).
[3]V. E. Demidov, S. Urazhdin, E. R. J. Edwards, and S. O. Demokritov, Appl. Phys. Lett. **99**, 172501 (2011).
[4]V. E. Demidov, S. Urazhdin, E. R. J. Edwards, M. D. Stiles, R. D. McMichael, and S. O. Demokritov, Phys. Rev. Lett **107**, 107204 (2011).
[5]Y. Kajiwara, K. Harii, S. Takahashi, J. Ohe, K. Uchida, M. Mizuguchi, H. Umezawa, H. Kawai, K. Ando, K. Takanashi, S. Maekawa, and E. Saitoh, Nature **464**, 262–266 (2010).
[6]Z. Wang, Y. Sun, M. Wu, V. Tiberkevich, and A. Slavin Phys. Rev. Lett. **107**, 146602 (2011).
[7]E. Padron-Hernandez, A. Azevedo, and S. M. Rezende, Appl. Phys. Lett. **99**, 192511 (2011).
[8]E. R. J. Edwards, H. Ulrichs, V. E. Demidov, S. O. Demokritov, and S. Urazhdin, Phys. Rev. B **86**, 134420 (2012).
[9]L. Liu, C.-F. Pai, D. C. Ralph, and R. A. Buhrman, Phys. Rev. Lett. **109**, 186602 (2012).
[10]V. E. Demidov, S. Urazhdin, H. Ulrichs, V. Tiberkevich, A. Slavin, D. Baither, G. Schmitz, and S. O. Demokritov, Nature Mater. **11**, 1028 (2012).
[11]R. H. Liu, W. L. Lim, and S. Urazhdin, Phys. Rev. Lett. **110**, 147601 (2013).
[12]M. I. Dyakonov and V. I. Perel, Sov. Phys. JETP Lett. **13**, 467 (1971).
[13]J. E. Hirsch, Phys. Rev. Lett. **83**, 1834 (1999).
[14]H. Kurebayashi, O. Dzyapko, V. E. Demidov, D. Fang, A. J. Ferguson, and S. O. Demokritov, Nature Mater. **10**, 660 (2011).
[15]H. Kurebayashi, O. Dzyapko, V. E. Demidov, D. Fang, A. J. Ferguson, and S. O. Demokritov, Appl. Phys. Lett. **99**, 162502 (2011).
[16]C. W. Sandweg, Y. Kajiwara, A. V. Chumak, A. A. Serga, V. I. Vasyuchka, M. B. Jungfleisch, E. Saitoh, and B. Hillebrands, Phys. Rev. Lett. **106**, 216601 (2011).
[17]V. Castel, N. Vlietstra, and B. J. van Wees, J. Ben Youssef, Phys. Rev. B **86**, 134419 (2012).
[18]C. Kittel, Phys. Rev. **73**, 155 (1948).
[19]C. W. Sandweg, Y. Kajiwara, K. Ando, E. Saitoh, and B. Hillebrands, Appl. Phys. Lett. **97**, 252504 (2010).
[20]E. Saitoh, M. Ueda, H. Miyajima, and G. Tatara, Appl. Phys. Lett. **88**, 182509 (2006).
[21]K. Harii, T. An, Y. Kajiwara, K. Ando, H. Nakayama, T. Yoshino, and E. Saitoh, J. Appl. Phys. **109**, 116105 (2011).
[22]K. Ando and E. Saitoh, J. Appl. Phys. **108**, 113925 (2010).
[23]B. A. Kalinikos, IEEE Proc., Part H: Microwaves, Antennas Propag. **127**, 4–10 (1980).